

Chemical modification of activated carbon surface with iron functional groups for efficient separation of vanadium: batch and column study

Hakimeh Shariffard¹ · Francesco Pepe² · Paolo Aprea³ · Bruno de Gennaro³

Received: 6 February 2017 / Accepted: 6 June 2017 / Published online: 16 June 2017
© Springer Science+Business Media B.V. 2017

Abstract In this study, iron functional groups-impregnated activated carbon (IIAC) composite was prepared as a novel adsorbent for vanadium separation. Adsorption experiments were performed in batch and column systems, and the effects of various operating parameters, such as solution pH, initial concentration, contact time, and temperature, were evaluated. The kinetic data confirmed the validity of the pseudo-second-order kinetic model for vanadium adsorption on IIAC. The sorption equilibrium data were analyzed using Langmuir, Freundlich, and Dubinin–Radushkevich isotherm models. The results showed that IIAC has a vanadium ions adsorption capacity of 313 mg g⁻¹. The activation and thermodynamic parameters were determined using kinetics and equilibrium data. The experimental data of the column adsorption process were fitted by Thomas and BDST models. The results showed that Thomas model can well describe the breakthrough curves. The column experiments showed that IIAC composite has good adsorption performance for vanadium ions adsorption.

Keywords Adsorption · Activated carbon · Impregnation · Iron functional groups · Vanadium

✉ Hakimeh Shariffard
hakimeh.sharifi@gmail.com

¹ Chemical Engineering Department, School of Engineering, Yasouj University, Yasuj, Iran

² Dipartimento di Ingegneria, Università del Sannio, Piazza Roma 21, 82100 Benevento, Italy

³ Dipartimento di Ingegneria Chimica, dei Materiali e della Produzione Industriale, Università Federico II, P.le Tecchio 80, 80125 Naples, Italy

Introduction

Heavy metals as the most common industrial pollutants are hazardous materials due to their toxic effects and tendency to bioaccumulation. One of these metals is vanadium, which is discharged to the environment through different industrial wastes such as steel slags, oil refineries wastes, and power-plant slags. The existence of vanadium in the environment has critical impacts on human health and environment [1–3]. Because of its toxicity, it is necessary to remove vanadium from industrial wastewater. Several processes have been investigated to this aim, including precipitation, extraction, membrane process, ion-exchange and adsorption [3–7]. Some of these processes have high capital and operational costs, and, furthermore, the management of residues originating from them is often complicated. The results of many types of research in this area show that the adsorption process has a significant potential for separation of heavy metal ions from aqueous solutions [8].

Activated carbon is an adsorbent material with a unique porous structure, high specific surface area and special chemical structure which can adsorb different kinds of contaminants from industrial wastes, but is characterized by a limited selectivity [9, 10]. Chemical modification of activated carbon surface to improve the selectivity of this material toward specific contaminants has attracted extensive interest. In particular, results of recent research works show that the impregnation of the activated carbon surface with iron functional groups leads to improvement of its adsorption properties and selectivity [11–13]. On the other hand, scarce literature data are available concerning the characterization of iron-impregnated activated carbon for vanadium removal, especially in fixed-bed column applications [14].

In our previous papers, we synthesized activated carbon/iron nanoparticles composites and tested them in a batch adsorption process for vanadium separation. In these works, Norit-activated carbons with different porous structure and chemical properties were treated with iron sulfate and iron chloride to prepare the nanocomposites [14, 15]. In order to overcome some weaknesses of the materials mentioned, in the present study a slightly different synthesis technique was used to prepare the iron-impregnated activated carbon (IIAC) composite: in particular, a commercial activated carbon based on coal, which is used in Khangiran gas refinery (Razavi Khorasan, Iran), was first oxidized with a concentrated HNO_3 solution, and then treated with iron nitrate. The novel composite was characterized and tested as a selective adsorbent for vanadium ions adsorption in batch and column processes. To the best of our knowledge, this paper is the first study addressing vanadium removal by adsorption in a fixed-bed column using the IIAC composite. Furthermore, a mass transfer modeling effort was undertaken to elucidate the role that different limiting steps play in the removal process. Particular emphasis was given to the comparison between adsorption capacities of IIAC and those of other materials, and to the regeneration characteristics of the synthesized sorbent.

Experimental

IIAC preparation

First, 15 g of commercial activated carbon was immersed in 200 mL of 60% HNO₃ (Merck) solution for 30 min at 30 °C. The oxidized activated carbon was rinsed with deionized water until the pH remained constant. Then, 10 g of dried pre-oxidized activated carbon was immersed in 200 mL of iron nitrate (Merck) solution with different iron concentrations (0.2–0.4–0.6 mol L⁻¹), and the suspension was shaken at a speed of 200 rpm for 24 h at 55 °C. After 24 h, the solid product was separated from the solution and washed several times with ultrapure water. The solid products synthesized at various iron concentrations were named IIAC0.2, IIAC0.4 and, IIAC0.6 composites, respectively. The composites were oven-dried at 60 °C for 1 day [14]. These adsorbents were used for vanadium adsorption together with non-functionalized commercial activated carbons in order to compare their performance. Vanadium removal experiments were carried out in a batch system at constant pH (4.5) and temperature (25 °C). Next, 0.05 g of adsorbent was added to 50 mL of vanadium solution (70 mg L⁻¹) and stirred at 200 rpm for 3 h. The pH of the solution was adjusted to pH 4.5 by adding NaOH and/or H₂SO₄ solutions (Merck). The adsorbent was separated at the end of stirring. The residual V concentration in the solution was determined using Inductively coupled plasma optical emission spectrometry (ICP-OES; Perkin Elmer Optima 2100 DV).

All the above-mentioned experiments were repeated two times, and the average values of removal percentages are reported in Table 1. The experimental results showed that the adsorption ability of commercial activated carbon was improved by impregnation with iron functional groups, and that IIAC0.6 has the highest adsorption capacity, being capable, in the experimental conditions considered, of removing almost 100% of vanadium after 3 h. Therefore, this sample was chosen for further experimentation. In order to ensure the accuracy and reproducibility of the data, we synthesized IIAC0.6 composite in duplicate and used these samples for vanadium separation. Our results showed that the synthesis process of the composite is reproducible.

Characterization

The textural properties of raw activated carbon and the IIAC0.6 composite were evaluated from N₂ adsorption–desorption isotherms at 77 K using an automatic volumetric system (Quantachrome NOVA 1000). Furthermore, in order to measure the pH_{ZPC} (point of zero charge) of the raw activated carbon and IIAC0.6, 50 mL of

Table 1 Adsorption ability of commercial activated carbon and prepared composites

Sample	Activated carbon	IIAC0.2	IIAC0.4	IIAC0.6
Vanadium removal %	65	83	90	100

0.1 N NaCl solution was poured into a set of glass containers. The initial pH of each NaCl solution was adjusted to a value in the range of 1–12 using 0.1 mol L⁻¹ HCl or NaOH solutions (Merck). Then, 0.1 g of adsorbent was added to each container and the containers were agitated for 48 h at 25 °C. At the end of this time, the solid was separated from the solution via filtration, and the final pH of the residual solutions was measured. The pH value such that initial and final pHs of the NaCl solution are equal is defined as pH_{ZPC} [16]. The chemical interaction of iron molecules with functional groups of activated carbon was studied by Fourier transform Infrared (FTIR) analysis using a Nicolet FTIR spectrophotometer NEXUS 670. The iron distribution on the IIAC0.6 surface was analyzed by energy-dispersive X-ray spectroscopy (EDS) and element mapping analysis (Tescan).

Batch adsorption of vanadium ions

In order to investigate the vanadium removal efficiency as a function of initial pH, adsorption experiments were performed at various initial pH values (1–9). In these experiments, initial vanadium concentration, the mass of adsorbent, agitation speed and temperature were 60 mg L⁻¹, 1 g L⁻¹, 250 rpm and 25 °C, respectively. After 3 h, the solid was separated via filtration and Energy-dispersive X-ray spectroscopy vanadium concentration in residual solution was determined using ICP-OES. Kinetic experiments were conducted as follows: 50 mL of vanadium solutions with initial concentration of 60 mg L⁻¹ and initial pH 4.5 were poured into glass Erlenmeyer flasks containing the IIAC0.6 composite (adsorbent dosage: 1 g L⁻¹). The flasks were shaken at 200 rpm for pre-selected times (5, 10, 15, 30, 45, 60, 90, 120, 180, and 240 min) at 25, 35 and 45 °C. After filtration, the vanadium concentration in the residual solutions was analyzed by ICP-OES and the amount of vanadium ions adsorbed by IIAC0.6, q , was calculated.

To determine the equilibrium isotherms, 0.05 g of IIAC0.6 was put into six Erlenmeyer flasks. Then, 50 mL vanadium ion solution at various initial concentrations (25, 50, 75, 100, 150, and 200 mg L⁻¹) were added to each flask. The initial pH of the vanadium solutions was 4.5. The flasks were shaken on an orbital shaker incubator at 200 rpm for 24 h at 25, 35, and 45 °C. The amount of vanadium ions adsorbed by IIAC0.6, q , was determined by analyzing the residual solutions after the filtration.

In order to ensure accuracy, all the batch adsorption experiments were performed in duplicate and the average values of two sets of data were used for adsorption calculation.

Column adsorption of vanadium ions

In order to evaluate the adsorption performance of the IIAC0.6 composite in dynamic conditions, the breakthrough curves of vanadium adsorption were determined in a glass column with an internal diameter of 0.9 cm and a length of 30 cm. Glass wool was placed at the inlet and outlet of the column to avoid any loss of adsorbent. A vanadium solution with known initial concentration and flowrate

was fed through the top of the column using a peristaltic pump (Pharmacia Fine Chemicals, P3 model) and the effluent was collected from the bottom of the column after preselected periods of time and analyzed using ICP-OES. Three adsorption/desorption cycles were performed, with the following process parameters: flowrate = 3.3 mL min⁻¹, inlet vanadium concentration = 100 mg L⁻¹, IIAC0.6 mass = 2.51 g.

The desorption of vanadium from IIAC0.6 bed was performed as follows: 0.2 M HCl solution was fed through the top of the column using a peristaltic pump for 48 h. The volumetric flowrate of HCl solution was 3.3 mL min⁻¹. After this time, the adsorbent bed was washed with ultrapure water until constant pH was reached.

To ensure the accuracy and reproducibility of the data, in all the column experiments samples were taken in duplicate, and analyzed using ICP-OES, and the average values of samples were considered in the calculations.

Results and discussion

Characterization of adsorbent

Specific surface area results and pH_{ZPC} of commercial activated carbon and IIAC0.6 are presented in Table 2. The decrease of specific surface area and pH_{ZPC} can be attributed to the formation of new iron functional groups on the activated carbon surface [14]. Figure 1 shows the FTIR spectra of commercial activated carbon and IIAC0.6. The assignments of the IR absorption bands are shown in Table 3 [14, 17–19]. The new IR absorption bands which appear in the IIAC0.6 spectrum reveal that iron molecules deposited on the carbon surface have a chemical interaction with the activated carbon functional groups, significantly modifying the surface chemistry of the synthesized nanocomposite with respect to the original activated carbon.

Figure 2a–c shows the EDS and element mapping of activated carbon and IIAC0.6 composites, respectively. These figures show the presence of iron on the surface of the composite, and, furthermore, element mapping indicates that the iron is homogeneously dispersed on the IIAC0.6 surface.

Effect of initial pH on vanadium removal

Figure 3a shows the effect of initial pH on the vanadium removal efficiency of the IIAC0.6 composite. The distribution diagram of vanadium species at various pH

Table 2 Chemical–physical properties of activated carbon and IIAC0.6

Adsorbent	BET surface area (m ² g ⁻¹)	Total pore volume (cm ³ g ⁻¹)	Average pore width, 4V _{tot} /S _{BET} (Å)	pH _{ZPC}
Activated carbon	927	0.589	25.415	6.8
IIAC0.6	690	0.441	25.565	5.4

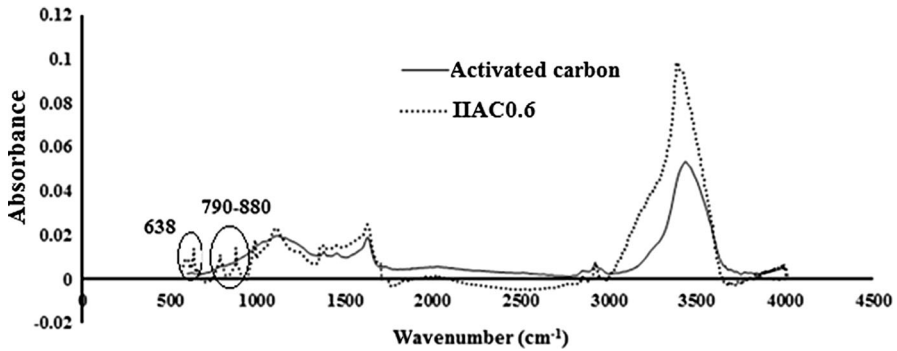


Fig. 1 FTIR spectra of commercial activated carbon and IIAC0.6 adsorbent

Table 3 Assignments of IR absorption bands for adsorbents [14, 17–19]

σ (cm ⁻¹)	Comments
3434, 3388	Hydroxyl groups (O-H)
2922–2930	C-H aliphatic stretching
2844–2850	-O-CH ₃ of the aldehyde group
1630	Stretching vibrations of C=O in carbonyl, lactone and carboxyl groups
1455	Stretching of C-O or O-H deformation in carboxylic acids
638	Formation of C-O-Fe bonds
790–880	Formation of Fe-O band

evaluated by Visual MINTEQ software v.3.0 is presented in Fig. 3b. According to Fig. 3a, the removal efficiency first increases when increasing the initial pH from 1 to 4, and then decreases when the pH is further increased from 4.5 to 9. The pH of the solution affects the surface charge of the adsorbent (IIAC0.6) and the chemical speciation of the adsorbate (vanadium). Figure 3b shows that vanadium mainly exists in the solution as cation (VO_2^+) when pH is lower than 3, while for $4 < \text{pH} < 11$, it mainly exists as anionic species [$\text{VO}_2(\text{OH})_2^-$ and $\text{VO}_3(\text{OH})^{2-}$] [20, 21]. Since pH_{ZPC} of adsorbent is 5.4, the low vanadium removal efficiency observed at $\text{pH} < 3$ can be attributed to repulsion between vanadium cations and the positively charged surface of IIAC0.6. At higher pH ($3.5 < \text{pH} < 5$), vanadium is present in solution mainly as anions, which can be adsorbed onto the positive surface of IIAC0.6. At even higher pH, ($\text{pH} > 5.5$), the surface of IIAC0.6 has a negative charge and therefore vanadium removal decreases [16].

Kinetic and activation parameters

The adsorption kinetics of vanadium onto IIAC0.6 were investigated by three common models, namely pseudo-first-order model, pseudo-second-order model and intraparticle diffusion model.

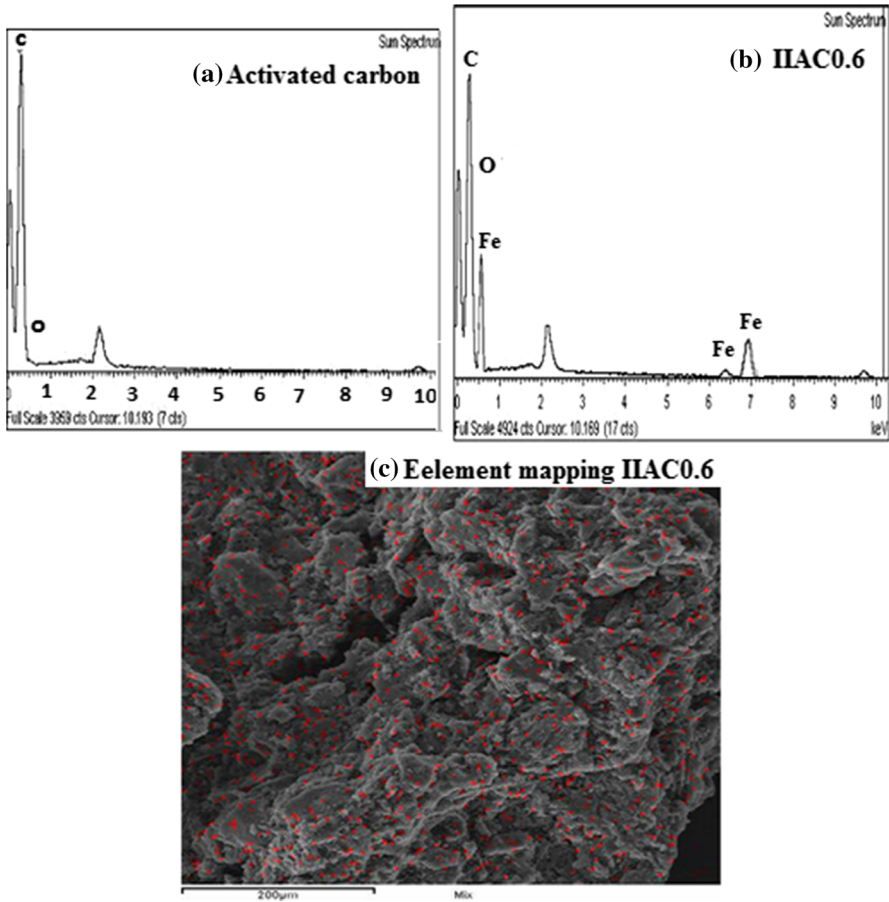


Fig. 2 a EDS analysis of activated carbon; b EDS analysis of IAC0.6; c element mapping of IAC0.6

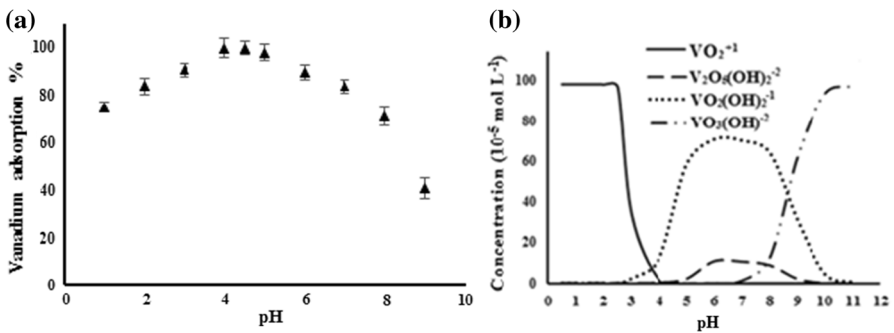


Fig. 3 a Removal efficiency of vanadium using IAC0.6 as a function of initial pH; b distribution diagram of vanadium species at various pH for an initial concentration 60 mg L^{-1}

The pseudo-first-order model assumes that the limiting step of the adsorption process is the physical interaction between adsorbate molecules (vanadium ions) and adsorbent active sites and that this interaction can be kinetically described by a first-order kinetic equation, with no role played by liquid–solid and intraparticle diffusion. If this model is appropriate, then the adsorption kinetics can be described by the following equation:

$$q_t = q_e(1 - e^{-k_1 t}) \quad (1)$$

where t is time (min), q_e and q_t are the amounts of vanadium adsorbed at equilibrium and at time t (mg g^{-1}), respectively, and k_1 is the rate constant for the adsorption (pseudo-) reaction (min^{-1}).

The experimental data were also analyzed by the pseudo-second-order model, which, once again, assumes that the overall process is limited by the chemical adsorbent–adsorbate interaction, which can be described by a second-order kinetic equation. In this case, the adsorption kinetics can be described as follows:

$$\frac{t}{q_t} = \frac{1}{k_2 q_e^2} + \frac{t}{q_e} \quad (2)$$

in which k_2 ($\text{g mg}^{-1} \text{min}^{-1}$) is the rate constant for the adsorption (pseudo-) reaction.

Eventually, the possibility that adsorption process is controlled by intraparticle diffusion was taken into account. If this is the case, then the adsorption kinetics can be described by the Morris–Weber model [22], according to which it is:

$$q_t = k_{\text{id}} t^{1/2} + \theta \quad (3)$$

in which k_{id} is the intraparticle diffusion rate constant, and θ is a constant which depends on the role played by external (fluid–solid) mass transfer.

The kinetic data relative to vanadium adsorption using IAC0.6 at three different temperatures are reported in Fig. 4. Parameters and R^2 values for the three models are reported in Table 4. Figure 4 indicates that there is a good agreement between the experimental data and the pseudo-second-order model. The R^2 values and the comparison between calculated and experimental values of q_e ($q_{e,\text{cal}}$ and $q_{e,\text{exp}}$, respectively) confirms that the experimental results are much better interpreted by the pseudo-second-order model than by the other models considered. This suggests that adsorption of vanadium on IAC0.6 is controlled by chemical reaction, and can be described by a second-order kinetic equation, with a negligible contribution of internal diffusion, at least in the experimental conditions considered.

Additionally, in order to evaluate the statistical meaningfulness of the parameters of the different kinetics models considered, the Chi squared test, F test and Student's t test were applied, and the results are presented in Table 5 [23, 24]. Results show that both Chi square test and F test are suitable to determine the best-fitting kinetics model which is also the pseudo-second-order model [23, 24].

In order to understand the mechanism of vanadium adsorption onto IAC0.6, the determination of mass transfer resistance is very important. The overall mass transfer resistance is dependent on either the external diffusion (film diffusion) or

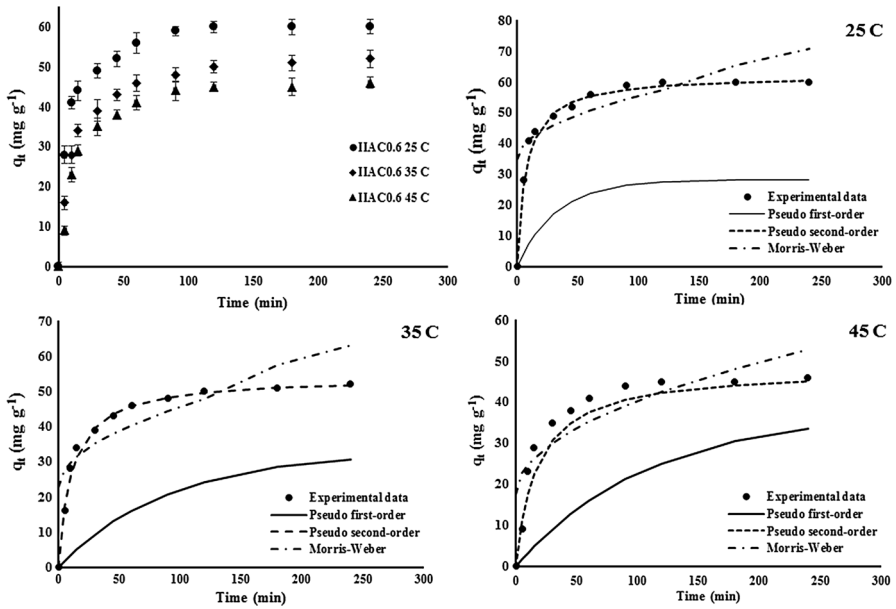


Fig. 4 Amount of vanadium adsorbed onto IAC0.6 as a function of time (min) at various temperatures

Table 4 Kinetics parameters for vanadium adsorption onto IAC0.6

Kinetic model	Parameter	25 °C	35 °C	45 °C
	$q_{e,exp}$ (mg/g)	60.00	52.00	46.00
Pseudo-first order	k_1	0.031	0.011	0.009
	$q_{e,cal}$	28.21	33.11	38.01
	R^2	0.920	0.870	0.830
Pseudo-second order	k_2	0.0022	0.0017	0.0012
	$q_{e,cal}$	62.29	54.05	48.28
	R^2	0.998	0.999	0.999
Morris-Weber model	k_{id}	2.06	2.30	2.28
	Θ	34.71	22.59	17.51
	R^2	0.740	0.77	0.71

the internal diffusion, or on both of them. The Fulazzaky mass transfer model was applied to describe the mass transfer resistance [14]. The most important mass transfer parameters including global mass transfer factor $[k_L a]_g$ (min^{-1}), external mass transfer factor $[k_L a]_f$ (min^{-1}) and internal mass transfer factor $[k_L a]_d$ (min^{-1}) were determined by mass transfer resistance analysis [14]. The following equation was applied to analyze the experimental data.

In this equation, B (mg g^{-1}) is the potential mass transfer index relating to the driving force of mass transfer and β (g min mg^{-1}) is the adsorbate-adsorbent affinity parameter.

Table 5 Kinetic error deviation estimation related to the vanadium adsorption onto IIAC0.6 using alternative statistical tools

Statistical tool	Temp. (°C)	Pseudo-first-order	Pseudo-second-order	Morris–Weber model
Chi square test	25	1.2631	95.8534	40.3067
	35	14.69011	30.87889	0.48792
	45	0.2043	90.9470	30.54747
<i>F</i> test	F	4.5578	46.8020	3.3897
	35	4.76356	96.0665	7.29910
	45	5.22497	76.04293	8.29524
<i>T</i> test	25	98.0970	5.70868	182.9354
	35	36.0365	1.72337	98.85471
	45	132.8877	17.1195	84.25279

The highest Chi square test, *F* test and *t* test values are in bold

$$q_t = B + \frac{1}{\beta} \ln(t) \quad (4)$$

The mass transfer parameters are calculated using the following equations:

$$= \begin{cases} B = \frac{\ln([k_L a]_g - \ln\left\{\ln\frac{C_0}{C_f}\right\})}{\beta} \\ [k_L a]_f = [k_L a]_g \times e^{-\beta q_t} \\ [k_L a]_d = [k_L a]_g - [k_L a]_f \end{cases} \quad (5)$$

where C_0 (mg L⁻¹) and C_f (mg g⁻¹) are the initial and final vanadium ions concentrations, respectively. Figure 5 shows the variation of $[k_L a]_g$, $[k_L a]_f$ and $[k_L a]_d$ versus C_f/C_0 . As can be seen, the curves for these mass transfer factors are comparable. It can be concluded that the overall mass transfer resistance is dependent on both the external and internal diffusions. Therefore, it can be said that both the external and internal diffusion steps are the rate controlling steps for vanadium adsorption from aqueous solution onto the IIAC0.6 surface.

The kinetics data obtained at different temperatures can be used to calculate the activation energy according to the Arrhenius equation [25]:

$$\ln k_2 = \ln A - \frac{E_a}{RT} \quad (6)$$

where E_a and A are the activation energy (kJ mol⁻¹) and the frequency factor in the Arrhenius equation (g gm⁻¹ min⁻¹), respectively. The activation energy for vanadium adsorption onto IIAC0.6 was -34.9 kJ mol⁻¹. The R^2 value for the linearized form of the Arrhenius equation was 0.965. The decreasing of the kinetic constant (k_2) with increasing temperature (Table 4) and the negative value of activation energy indicate the exothermic nature of vanadium adsorption using IIAC0.6.

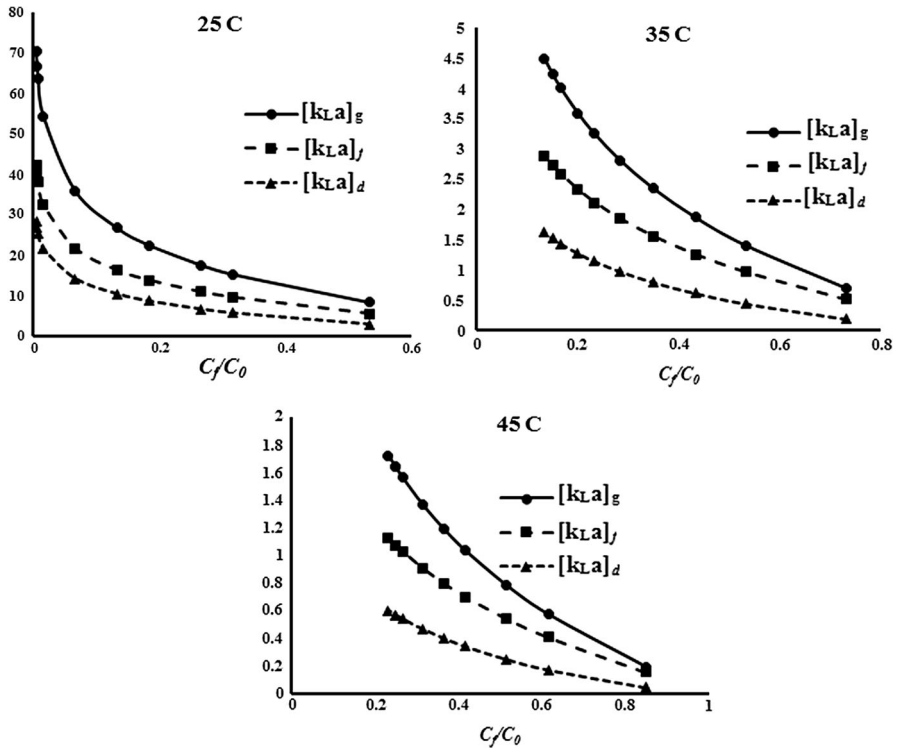


Fig. 5 Variation of mass transfer factors at different temperature

Adsorption equilibrium

The equilibrium data relative to vanadium adsorption on IIAC0.6 at 25, 35 and 45 °C are reported in Fig. 6. In order to have a clearer understanding of the adsorption process, the available data were fitted using the Langmuir, Freundlich and Dubinin–Radsuskevich isotherms. The Langmuir isotherm is based on the assumptions that all the adsorption sites are equivalent for what concerns adsorbent–adsorbate interactions, that each site only interacts with a single adsorbate molecule/ion and that adsorbate–adsorbate interactions are negligible. The Langmuir isotherm equation is described by the following equation:

$$q_e = q_{\max} \frac{K_L C_e}{1 + K_L C_e} \tag{7}$$

where C_e (mg g^{-1}) is the equilibrium concentration of adsorbate and K_L (L mg^{-1}) and q_{\max} (mg g^{-1}) are the model parameters: q_{\max} represents the maximum amount of adsorbate which can be theoretically adsorbed per unit mass of adsorbent when the monolayer coverage is complete, while K_L is a measure of adsorbent–adsorbate affinity.

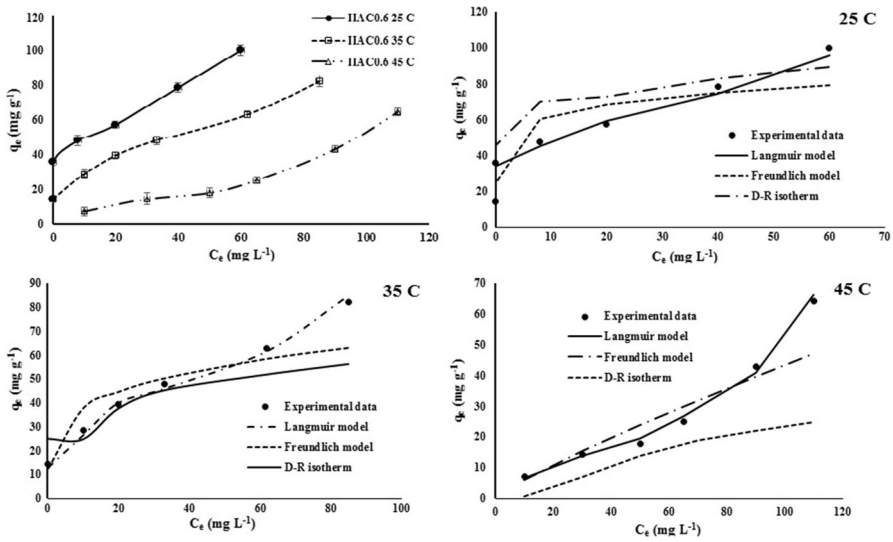


Fig. 6 Adsorption isotherms of vanadium at various temperatures

The Freundlich isotherm is an essentially empirical equation, which assumes that the adsorption process takes place on a heterogeneous surface, and is described by the following equation:

$$q_e = K_f(C_e)^{1/n} \quad (8)$$

where K_f and n are the model parameters. K_f ($\text{mg g}^{-1} \text{L}^{1/n} \text{mg}^{-1/n}$) is an indicator of the adsorption capacity of the adsorbent and n is a measure of the favorability of adsorption.

The Dubinin–Radushkevich (D–R) isotherm, eventually, is a model originally proposed to describe gas-phase adsorption of subcritical vapors on porous sorbents, and can in general be used to describe adsorption on a heterogeneous surface characterized by a Gaussian distribution of adsorbent–adsorbate interaction energy. The D–R equation is described as follows:

$$q_e = q_{\max} \exp \left[-\frac{1}{2} \left(\frac{\varepsilon}{E} \right)^2 \right] \quad \varepsilon = RT \ln \left(1 + \frac{1}{C_e} \right) \quad (9)$$

where R and T are the gas constant ($\text{kJ mol}^{-1} \text{K}^{-1}$) and absolute temperature (K), respectively, and q_{\max} (mol g^{-1}) and E (kJ mol^{-1}) are the model parameters. As indicated above, q_{\max} represents the maximum possible amount of adsorbate; E , on the other hand, is the mean free energy of adsorption per mole of adsorbate when it is transferred to the surface of solid from infinity in the solution.

In order to compare the three isotherm models considered, the optimal values of the parameters were estimated starting from the linearized forms of Eqs. (7–9). The results of the regressions, together with the regression coefficients R^2 , are presented in Table 6.

Figure 6 and the comparison among the different regressions indicates that the Langmuir model can well describe the experimental data, suggesting that vanadium adsorption on IIAC0.6 takes place as a monolayer adsorption process. The values of E (KJ mol^{-1}) are consistent with those typical of ion-exchange processes and electrostatic attraction (chemical sorption) [26].

Table 7 presents the calculated values of the Chi square test, F test, and t test for the isotherm models at different temperatures. The results show that the F test and the t test are suitable for determining the most appropriate fitting-model, which is the Langmuir isotherm model.

The maximum adsorption capacity of IIAC0.6 was 313 mg g^{-1} , which compares very favorably with the vanadium adsorption capacities of other sorbents reported in the literature, as shown in Fig. 7 [26–39]. This remarkably high capacity of the IIAC0.6 composite for vanadium removal can be attributed to the creation of new functional groups on the activated carbon surface. This functional groups have iron ions that have positive charge and can adsorb vanadium via electrostatic attraction. According to the FTIR spectra, these are new functional groups such as C–O–Fe and O–Fe on the IIAC0.6 surface. Figure 8 illustrates the possible mechanisms for vanadium removal using the IIAC0.6 composite.

Furthermore, it is interesting to observe that both the maximum adsorption capacity q_{max} and the affinity constant K_L significantly decrease with temperature. Concerning K_L , its dependence on temperature was used to determine the thermodynamic parameters such as ΔG° , ΔH° and ΔS° according to the following equations:

$$\begin{cases} \Delta G^\circ = -RT \ln K_L \\ \ln K_L = -\frac{\Delta H^\circ}{RT} + \frac{\Delta S^\circ}{R} \\ T\Delta S^\circ = \Delta H^\circ - \Delta G^\circ \end{cases} \quad (10)$$

ΔH° and ΔS° can be obtained as the slope and intercept of a plot of $\ln(K_L)$ versus $1/T$.

In particular, it turned out that $\Delta H^\circ = -28.6 \text{ kJ mol}^{-1}$ and $\Delta S^\circ = -0.047 \text{ kJ mol}^{-1} \text{ K}^{-1}$. The results show that the value of ΔG° decreased

Table 6 Langmuir, Freundlich and D–R isotherm constant parameters

Isotherm	Parameters	25 °C	35 °C	45 °C
Langmuir	q_{max} (mg g^{-1})	312.50	114.16	111.101
	K_L (L mg^{-1})	0.0074	0.0042	0.0036
	R^2	0.997	0.996	0.978
Freundlich	K_f	98.19	109.30	10.22
	n	3.84	2.70	1.16
	R^2	0.852	0.910	0.917
D–R	E (kJ mol^{-1})	15.811	13.608	7.905
	q_{max} (mol g^{-1})	0.0029	0.0022	0.0009
	R^2	0.958	0.835	0.802

Table 7 Equilibrium isotherm error deviation estimation related to the vanadium adsorption onto IIAC0.6 using alternative statistical tools

Statistical tool	Temp. (°C)	Langmuir	Freundlich	D-R
Chi square test	25	1.84422	15.8645	0.00230
	35	0.4717	9.36131	0.00022
	45	0.431204	9.13586	0.02328
<i>F</i> test	25	55.1662	16.16523	2.70974
	35	76.0266	12.94631	8.71399
	45	71.601	12.81332	2.59565
<i>T</i> test	25	38.2801	16.64850	1.47454
	35	16.92764	6.10032	5.55133
	45	15.23802	4.39533	7.19642

The highest Chi square test, *F* test and *t* test values are in bold

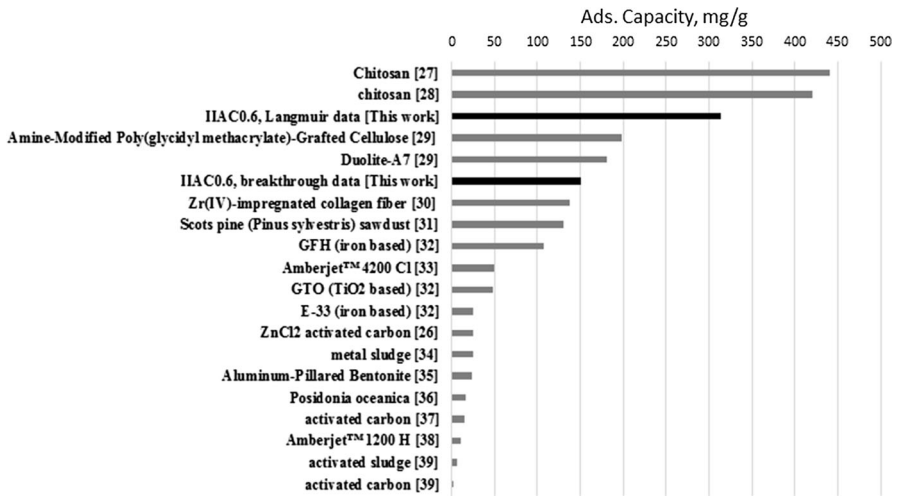


Fig. 7 Comparison of vanadium adsorption capacity of different adsorbents with those of this work [26–39]

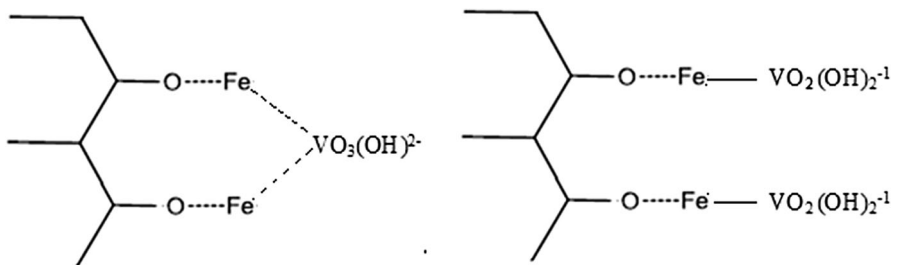


Fig. 8 Schematic of adsorption mechanism of vanadium ions by IIAC0.6 adsorbent

from -14.7 to -13.8 kJ mol^{-1} when the temperature increased from 25 to 45 $^{\circ}\text{C}$ for vanadium adsorption using IIAC0.6. The negative value of ΔH° confirms that vanadium adsorption on IIAC0.6 is an exothermic phenomenon.

Vanadium adsorption in fixed-bed column

The adsorption performance of a fixed-bed column is conveniently evaluated via its adsorption breakthrough curve (dimensionless bulk concentration C_{out}/C_0 vs. time). The two important characteristics used to describe the adsorption performance of a fixed-bed column are the total amount of adsorbed vanadium (q_{total} , mg) and the breakthrough time (min), i.e. the time required to reach $C_{\text{out}}/C_0 = 0.05$. In general, a process which has higher performance adsorbs a higher amount of vanadium and has a higher breakthrough time. Figure 9 shows the breakthrough curves of vanadium adsorption using IIAC0.6 at three adsorption/desorption cycles.

The breakthrough time for each run is obtained from experimental breakthrough curves, and the total amount of vanadium adsorbed onto the IIAC0.6 bed is calculated from the following equation [40]:

$$q_{\text{total}} = QA = Q \int_0^{t_{\text{total}}} (C_0 - C_{\text{out}}) dt \quad (11)$$

where Q (L min^{-1}), C_0 (mg L^{-1}) and C_{out} (mg L^{-1}) are the flowrate, inlet vanadium concentration and outlet vanadium concentration after passing the column, respectively. Table 8 presents the breakthrough time ($t_{0.05}$) and the total amount of vanadium adsorbed in the column ($t_{0.05}$ and q_{total}) for three cycles. These results show that IIAC0.6 has a good adsorption performance for vanadium adsorption in a fixed-bed column after three cycles. The breakthrough time and the total amount of vanadium adsorbed using IIAC0.6 in the first cycle were 660 min and 356 mg, respectively. The experimental adsorption capacity of the fixed-bed column, q_{eq} (mg g^{-1}), is calculated as follows:

$$q_{\text{eq}} = \frac{q_{\text{total}}}{m} \quad (12)$$

The breakthrough curves were analyzed using Thomas and Bed Depth Service Time (BDST) models. The Thomas model is one of the most general models in column performance analysis and is largely applied to determine the adsorption

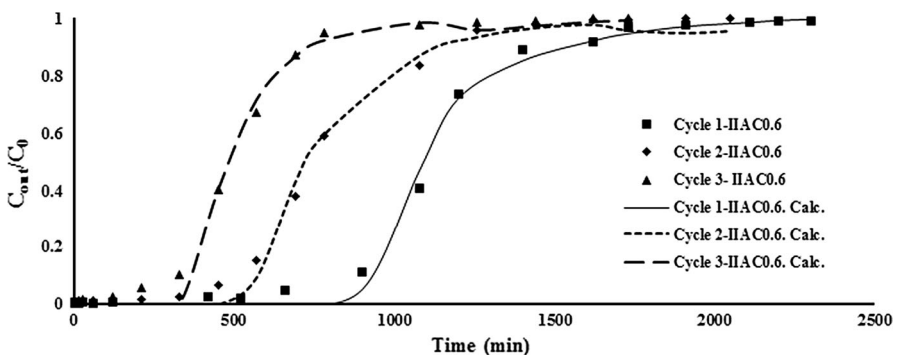


Fig. 9 Breakthrough curves of vanadium adsorption by IIAC0.6 in three adsorption cycles (Points experimental data; lines Thomas model predictions)

Table 8 Breakthrough time, total amount and experimental adsorption capacity

Parameter	Cycle 1	Cycle 2	Cycle 3
Breakthrough time ($t_{0.05}$) (min)	660	435	200
q_{total} (mg)	356.671	262.30	167.16
q_{eq} (mg g ⁻¹)	142.10	104.50	66.59

capacity of adsorbent and predict the breakthrough curves [41]. This model assumes the Langmuir isotherm and the second-order reversible reaction kinetics [42, 43], and is described by the following equation:

$$\frac{C_{\text{out}}}{C_0} = \frac{1}{1 + \exp\left[\frac{k_{\text{Th}}}{Q}(q_F m - C_0 Q t)\right]} \quad (13)$$

In this equation, k_{Th} (L min⁻¹ mg⁻¹) and q_F (mg g⁻¹) are the Thomas rate constant and sorption capacity of the adsorbent in the column system, respectively, and Q (L min⁻¹) and m (g) are the volumetric flowrate and mass of adsorbent in the column, respectively. A plot of $\ln[(C_0/C_{\text{out}}) - 1]$ versus time (min) is used to determine the k_{Th} and q_F .

The BDST model is a simple and widely used model that relates bed height (H) to service time (t) in terms of process parameters [44, 45]. This model is given as follows:

$$\frac{C_{\text{out}}}{C_0} = \frac{1}{1 + \exp\left[k_{\text{BDST}} C_0 \left(\frac{q_m}{u C_0} H - t\right)\right]} \quad (14)$$

where k_{BDST} (L min⁻¹ mg⁻¹) is the rate constant for the model, q_m (mg L⁻¹) is the adsorption capacity of adsorbent and u (cm min⁻¹) is the linear velocity of solution through the bed and calculated by Q/A , A being the sectional area of column. The model parameters, k_{BDST} and q_m can be determined from a plot of $\ln[(C_0/C_{\text{out}}) - 1]$ versus time.

The Thomas and BDST parameters are presented in Table 9 for the breakthrough curves of vanadium adsorption using IAC0.6 in three cycles. The R^2 values of the Thomas model are sufficient and the calculated q_F from the Thomas model is closely similar to the experimental value of q_{eq} . These results show the validity of this model to predict the breakthrough curves of vanadium adsorption using IAC0.6. These data also show that IAC0.6 has a comparable sorption capacity for

Table 9 Thomas and BDST model parameters for vanadium adsorption in IAC0.6 bed

Cycle	Thomas			BDST		
	k_{Th}	q_F	R^2	k_{BDST}	q_m	R^2
Cycle 1	4.5×10^{-5}	150.72	0.940	2.173	220	0.94
Cycle 2	6.43×10^{-5}	103.01	0.989	1.562	201	0.971
Cycle 3	7.57×10^{-5}	68.80	0.978	1.333	169	0.952

vanadium adsorption in the fixed-bed column [34]. Also, the data in Table 9 indicate that the sorption capacity of IIAC0.6 after three cycles is good. This result suggests a very high regenerability of the proposed material for vanadium adsorption in a fixed-bed system. The results show that the IIAC0.6 can be an excellent adsorbent for practical application in the vanadium separation from industrial wastewater, such as aqueous solutions after leaching the steel slags.

Conclusions

A novel composite material obtained by impregnating activated carbon with iron functional groups, IIAC0.6, was prepared by oxidizing a commercial activated carbon with concentrated HNO_3 and then by functionalizing it with iron nitrate. Characterization tests indicated that IIAC0.6 retained a high porosity and that new iron functional groups are created and distributed onto an activated carbon surface.

Kinetics and thermodynamics of vanadium adsorption on IIAC0.6 from aqueous solutions have been thoroughly studied. Adsorption kinetics are controlled by the adsorption pseudo-reaction rather than intraparticle diffusion, and that this pseudo-reaction can be described by a second-order kinetic equation. The Langmuir isotherm satisfactorily describes the equilibrium adsorption of vanadium on IIAC0.6. The results show that this process has a markedly chemical nature, and that the maximum adsorption capacity of IIAC0.6 is 313 mg g^{-1} . The comparison between the adsorption capacity exhibited by IIAC0.6 and the capacities reported in the literature for other adsorbing materials is very favorable. Furthermore, IIAC0.6 exhibits a good adsorption performance for vanadium adsorption in a column system, with a high regenerability. Based on this analysis, the IIAC0.6 adsorbent can be an excellent candidate for practical applications in the removal of vanadium from wastewater.

Acknowledgement The authors wish to acknowledge the Ministry for Foreign Affairs and International Cooperation of Italy for Financial support.

References

1. H. Wyers, *Brit. J. Ind. Med.* **3**, 177–182 (1946)
2. B. Patel, G.E. Henderson, S.J. Haswell, R. Grzeskowiak, *The Analyst* **115**, 1063–1066 (1990)
3. A.P. Rodríguez, J.A.H. Viezcas, J.R.P. Videá, G.L.G. Torresdey, O.P. Pérez, F.R.R. Velázquez, *Microchem. J.* **118**, 1–11 (2015)
4. A. Dabrowski, Z. Hubicki, P. Podkościelny, E. Robens, *Chemosphere* **56**, 91–106 (2004)
5. A. Alibrahim, H. Shlewit, S. Alike, *Chem. Eng. J.* **52**(1), 29–33 (2008)
6. M. Nabavinia, M. Soleimani, A. Kargari, *Int. J. Chem. Environ. Eng.* **3**, 149–152 (2012)
7. R. Navarro, J. Guzman, I. Saucedo, J. Revilla, E. Guibal, *Waste Manag.* **27**, 425–438 (2007)
8. N. Mehrabi, M. Soleimani, M.M. Yeganeh, H. Sharififard, *RSC Adv.* **5**, 51470–51482 (2015)
9. R. Chand-Bansal, M. Goyal, *Activated Carbon Adsorption* (Taylor & Francis, Boca Raton, 2005)
10. H. Marsh, F. Rodríguez-Reinoso, *Activated Carbon* (Elsevier, New York, 2006)
11. A.M. Cooper, K.D. Hristovski, T. Möller, P. Westerhoff, P. Sylvester, *J. Hazard. Mater.* **183**, 381–388 (2010)
12. J.A. Arcibar-Orozco, J.R. Rangel-Mendez, T.J. Bandoz, *J. Hazard. Mater.* **246–247**, 300–309 (2013)
13. J.H. Xu, N. Gao, Y. Deng, S. Xia, *Chem. Eng. J.* **222**, 520–526 (2013)

14. H. Shariffard, M. Soleimani, *RSC Adv.* **5**, 80650–80660 (2015)
15. H. Shariffard, M. Soleimani, *Res. Chem. Intermed.* **43**, 2501–2516 (2017)
16. H. Shariffard, F. Zokae Ashtiani, M. Soleimani, *Asia Pac. J. Chem. Eng.* **8**, 384–395 (2013)
17. P. Cambier, *Clay Miner.* **21**, 191–200 (1986)
18. Z. Al-Qodah, R. Shawabkah, *Braz. J. Chem. Eng.* **26**, 127–136 (2009)
19. Y. Li, C. Zhu, T. Lu, Z. Guo, D. Zhang, J. Ma, S. Zhu, *Carbon* **52**, 565–573 (2013)
20. T.S. Anirudhan, P.G. Radhakrishnan, *Chem. Eng. J.* **165**, 142–150 (2010)
21. T. Wang, Z. Cheng, B. Wang, W. Ma, *Chem. Eng. J.* **181–182**, 182–188 (2012)
22. B.H. Hameed, A.A. Ahmad, *J. Hazard. Mater.* **164**, 870–875 (2009)
23. M.C. Ncibi, *J. Hazard. Mater.* **153**, 207–212 (2008)
24. K. Riahi, S. Chaabane, B.B. Thayer, *J. Saudi Chem. Soc.* **21**, 143–152 (2017)
25. V.J. Inglezakis, A.A. Zorpas, *Desalin. Water Treat.* **39**, 149–157 (2012)
26. C. Namasivayam, D. Sangeetha, *Adsorption* **12**, 103–117 (2006)
27. J. Guzman, I. Saucedo, R. Navarro, J. Revilla, E. Guibal, *Langmuir* **18**, 1567–1573 (2002)
28. M. Jansson-Charrier, E. Guibal, J. Roussy, B. Delanghe, P. Le Cloirec, *Water Res.* **30**, 465–475 (2002)
29. T.S. Anirudhan, S. Jalajamony, L. Divya, *Ind. Eng. Chem. Res.* **48**, 2118–2124 (2009)
30. X.P. Liao, W. Tang, R.Q. Zhou, B. Shi, *Adsorption* **14**, 55–64 (2008)
31. T. Leiviskä, A. Keränen, N. Vainionpää, J. Al Amir, O. Hormi, J. Tanskanen, *Water Sci. Technol.* **72**, 437–442 (2015)
32. A. Naeem, P. Westerhoff, S. Mustafa, *Water Res.* **41**, 1596–1602 (2007)
33. M. Govindaraj, S. Pattabhi, *Desalin. Water Treat.* **54**, 2664–2674 (2015)
34. A. Bhatnagar, A.K. Minocha, D. Pudasainee, H.K. Chung, S.H. Kim, H.S. Kim, G. Lee, B. Min, B.H. Jeon, *Chem. Eng. J.* **144**, 197–204 (2008)
35. D.M. Manohar, B.F. Noeline, T.S. Anirudhan, *Ind. Eng. Chem. Res.* **44**, 6676–6684 (2005)
36. C. Pennesi, C. Totti, F. Beolchini, *PLoS ONE* **8**(10), e76870 (2013)
37. A. Keränen, T. Leiviskä, A. Salakka, J. Tanskanen, *Desalin. Water Treat.* **53**, 2645–2654 (2015)
38. Y. Shi, J. Yang, W. Mao, Y. Li, X. Xu, H. Zhang, W. Yu, Y. Li, C. Yang, *Desalin. Water Treat.* **53**, 2655–2663 (2015)
39. R.G. Kunz, J.F. Giannelli, H.D. Stensel, *J. Water Pollut. Control Feder.* **48**, 762–770 (1976)
40. M. Songolzadeh, M. Soleimani, M. Takht Ravanchi, *J. Nat. Gas Sci. Eng.* **27**, 831–841 (2015)
41. R. Han, Y. Wang, W. Yu, W. Zou, J. Shi, H. Lui, *J. Hazard. Mater.* **139**, 513–518 (2006)
42. M. Ghasemi, A.R. Keshtkar, R. Dabbagh, S. Jaber Safdari, *J. Hazard. Mater.* **189**(1–2), 141–149 (2011)
43. Z. Xu, J.G. Cai, B.C. Pan, *J. Zhejiang Univ. Sci. A* **14**, 155–176 (2013)
44. G.S. Bohart, E.Q. Adams, *J. Chem. Soc.* **42**, 523–529 (1920)
45. A.B. Albadarin, C. Mangwandi, A.H. Al-Muhtaseb, G.M. Walker, S.J. Allen, M.N.M. Ahmad, *Chin. J. Chem. Eng.* **20**(3), 469–477 (2012)